Psychoneuroendocrinology 107 (2019) 59–69

Contents lists available at ScienceDirect

Psychoneuroendocrinology

journal homepage: www.elsevier.com/locate/psyneuen

Chronic mild stress leads to aberrant glucose energy metabolism in depressed *Macaca fascicularis* models

Yinhua Qin[a,b,c,1], XiaoFeng Jiang[a,b,d,1], Wei Li[e,1], Jie Li[f,1], Tian Tian[a,b,d], Guangchao Zang[b,h], Liang Fang[g], Chanjuan Zhou[g], Bin Xu[a,b,d], Xue Gong[a,b,d], Cheng Huang[a,b,d], Xun Yang[a,b,d], Mengge Bai[a,b,c], Li Fan[a,b,d], Peng Xie[a,b,d,*]

[a] *Institute of Neuroscience and the Collaborative Innovation Center for Brain Science, Chongqing Medical University, Chongqing 400016, China*
[b] *Chongqing Key Laboratory of Neurobiology, Chongqing 400016, China*
[c] *Key Laboratory of Laboratory Medical Diagnostics of Education, Department of Laboratory Medicine, Chongqing 400016, China*
[d] *Department of Neurology, The First Affiliated Hospital of Chongqing Medical University, Chongqing 400016, China*
[e] *Department of Neurology, Army Medical Center of PLA, Chongqing 400042, China*
[f] *Clinical Medicine Research Center, Dazhou Central Hospital, Sichuan 635000, China*
[g] *Department of Neurology, Yongchuan Hospital, Chongqing Medical University, Chongqing 402460, China*
[h] *Laboratory of Tissue and Cell Biology, Lab Teaching & Management Center of Chongqing Medical University, Chongqing 400016, China*

ARTICLE INFO

Keywords:
Major depressive disorder
Naturally occurring depression
Energy metabolism
i-TRAQ
Cynomolgus

ABSTRACT

Background: Major depressive disorder (MDD) is a pathophysiologically uncharacterized mental illness with complex etiology and clinical manifestations. Rodent depression-like models have been widely used to mimic the morbid state of depression. However, research on emotional disorders can also benefit from the use of models in non-human primates, which share a wide range of genetic and social similarities with humans.

Methods: To investigate the pathophysiological mechanisms of depression, we established two models, naturally occurring depression cynomolgus (NOD) and social plus visual isolation-induced depression cynomolgus (SVC), imitating chronic mild or acute intense stress, respectively. We used i-TRAQ (isobaric tags for relative and absolute quantitation)-based quantitative proteomics and shotgun proteomics to identify differentially expressed proteins in cerebrospinal fluid (CSF) of the two monkey models and human MDD patients. We also used DAVID and ingenuity pathway analysis (IPA) for further bioinformatic investigation.

Results: In behavioral tests, NOD monkeys achieved higher scores in depression-like and anxiety-like behavioral measures, and spent more time on ingesting, thermoregulatory, and locomotive actions than SVC monkeys. A total of 902 proteins were identified by i-TRAQ, and 40 differentially expressed proteins were identified in each of the NOD-CON1 and SVC-CON2 groups. Application of DAVID revealed dysregulation of energy metabolism in the NOD group, whereas lipid metabolism and inflammatory response pathways were significantly altered in the SVC group. Use of IPA and Cytoscape showed that the oxygen species metabolic process glycolysis I/gluconeogenesis I, accompanied by downregulation of tubulin beta 3 class III (TUBB3), RAC-alpha serine/threonine-protein kinase (AKT1), and glyceraldehyde-3-phosphate dehydrogenase (GAPDH), was the most significantly affected pathway in the NOD group. Furthermore, 152 differentially expressed proteins in human MDD patients also revealed disruption of glucose energy metabolism. Significantly aberrant energy metabolism in various brain regions and the plasma and liver of chronic unpredictable mild stress rodent samples were also observed in a previous study.

Conclusions: Our results reveal for the first time the overall CSF protein profiles of two cynomolgus monkey models of depression. We propose that chronic mild stress may affect the disruption of glucose energy metabolism in NOD cynomolgus monkeys and rodents. These findings promote our understanding of the pathophysiology of MDD and may help to identify novel therapeutic targets.

---

[*] Corresponding author at: Department of Neurology and Psychiatry, The First Affiliated Hospital of Chongqing Medical University, No. 1 Yixueyuan Road, Chongqing, 400016, China.

E-mail address: xiepeng@cqmu.edu.cn (P. Xie).

[1] These authors contributed equally to this study.

https://doi.org/10.1016/j.psyneuen.2019.05.007
Received 20 December 2018; Received in revised form 5 May 2019; Accepted 9 May 2019

1. Introduction

Major depressive disorder (MDD) is a mental disease mainly characterized by hopelessness, anhedonia, and even suicide attempts, affecting more than 300 million people worldwide according to the World Health Organization (WHO). Recent studies have indicated that the hypothalamic–pituitary–adrenal (HPA) axis and autonomic nervous system (ANS) function, signaling, and synapse elimination and plasticity are altered in depression both *in vitro* and *in vivo*, but the underlying pathological mechanisms of MDD remain unclear (Gomez et al., 2017; van Dammen et al., 2018; Voleti et al., 2012). Rodent depression-like models (e.g., rats and mice) have been widely used to mimic the morbid state of depression for the purpose of identifying therapeutic targets (Cui et al., 2018; Loh et al., 2018). However, these models do not accurately approximate the etiopathological development of depression in humans that occurs naturally in a social context (Xu et al., 2015).

In view of the above limitations of rodents, non-human primates have been increasingly used in brain research (Fox et al., 2010). Primatology research suggests that other primates can suffer from crippling depression or anxiety, implying that these conditions may not be unique to humans (Shively et al., 2002). Social stress-associated behavioral depression in adult female cynomolgus macaques closely resembles human depression in its behavioral, neurobiological, and physiological characteristics (Shively, 2011). Carol A. Shively designed the first experimental study screening for social subordination, which showed that the stress of social subordination causes HPA and ovarian dysfunction, supporting the hypothesis that chronic, low-intensity social stress may result in depression in susceptible individuals (Laber-Laird and Anton, 1997). Social isolation has also been used to construct cynomolgus macaque models of depression (Shively et al., 2005). Nevertheless, there are only a few institutions that are allowed to conduct primate research because of strict ethical requirements. We previously reported that macaques exhibit naturally occurring depression similar to that in humans, and proposed a non-human primate depression model in a realistic social ethological context that can better approximate the psychosocial stressors underlying depression in humans (Li et al., 2013; Xu et al., 2015).

Analysis of cerebrospinal fluid (CSF), which contains proteins, signaling peptides, small signaling molecules, metabolic enzymes, metabolites, and other cellular products and is in direct contact with the central nervous system (CNS), can provide insights into neurological and psychiatric disorders (Brent et al., 2015; Reynolds et al., 2016; Tsuchimine and Kunugi, 2018). Using isobaric tags for relative and absolute quantitation (i-TRAQ) combined with liquid chromatography (LC) and tandem mass spectrometry (MS/MS), it is possible to construct data-driven systems biology models from high-throughput data sets, thereby increasing the possibility of identifying less abundant proteins in CSF. We previously performed i-TRAQ-based proteomic analysis of plasma from MDD patients and brain or liver from depressed rodents (Bai et al., 2018; Guo et al., 2018; Liu et al., 2018; Zeng et al., 2018). Combined proteomic and metabolomic analysis provided strong evidence that patients with mood disorders exhibit disruptions in energy metabolism, lipid metabolism, and immunoregulation, which are associated with an increased risk for the development of pathogenesis.

In the present study, we applied i-TRAQ, followed by LTQ-Orbitrap Velos mass spectrometry, shotgun protein identification, and bioinformatic analysis, to determine changes in differentially expressed proteins and elucidate the possible molecular pathways involved in major depression in monkeys and humans. We investigated the behavior of naturally occurring depression (NOD) cynomolgus and social plus visual isolation-induced depression cynomolgus (SVC) monkeys, and analyzed their CSF proteomes [NOD vs. control (CON1); SVC vs. control (CON2)] by i-TRAQ. We screened the differentially expressed proteins, and determined the associated pathways and functions using DAVID, ingenuity pathway analysis (IPA), and Cytoscape bioinformatic analysis. We then compared the affected signaling and disease pathways among the groups, the results of which could aid in further exploration of the pathophysiology underlying CSF dysfunction in primate-based depression-like models.

2. Material and methods

2.1. Ethical considerations

The Ethics Committee of Chongqing Medical University reviewed and approved the protocols of this study and the procedures employed for sample collection and analysis. All subjects gave their written informed consent after reading a detailed introduction to the study. All procedures were performed in accordance with the Helsinki Declaration.

All animal work was conducted in accordance with relevant national and international guidelines, such as the National Institutes of Health Guide for the Care and Use of Laboratory Animals (NIH Publication No. 8023, revised 1978). This study was performed in strict accordance with the recommendations in the Guide for the Care and Use of Laboratory Animals of the Institute of Neuroscience at Chongqing Medical University (approval no. 20,100,031).

2.2. Subjects and samples

The cerebrospinal fluid (CSF) of 16 adult depression patients (MDD) and 16 healthy adults (HC) was

collected at the Department of Psychiatry and the Medical Examination Center of the First Affiliated Hospital of Chongqing Medical University, respectively. The inclusion criteria for the patients were as follows: 1) Hamilton Depression Rating Scale (HAM-D) score ≥30, before antidepressant therapy; 2) no comorbidity of schizophrenia or neurological diseases and no significant abnormalities in the results of clinical laboratory tests (blood and urine examinations, liver function tests); 3) and age ≥18. All participants were interviewed with the Structured Clinical Interview for DSM-IV. Lumbar puncture was performed upon admission at the fourth lumbar intervertebral space using an atraumatic needle with local anesthesia, with the subject in a lateral position. A total of 1 ml of CSF was collected and subjected to centrifugation for 15 min at 3000 ×*g*; the liquid supernatant obtained was then stored at −80 °C. All human CSF samples were mixed within each group (*i.e.*, MDD and HC).

The cynomolgus monkey feeding base at Zhongke Experimental Animal Co., Ltd. (hereafter “Zhongke”), is located in Suzhou, China. All subjects were obtained from Zhongke with the permission of SYXK (SU) 2002-0032. From the original population (n = 6012), 52 candidate subjects were selected using a set of screening principles, and were assigned to four groups: a NOD group containing 16 female adult monkeys, with 16 female subjects in the corresponding healthy control group (CON1); and an SVC group containing 10 female monkeys, with 10 female monkeys in the no isolation control group (CON2). After the depression model procedures, 1 ml of CSF was collected from the lumbar spine after the intramuscular injection of 1% ketamine (6 ml/kg). After centrifugation for 15 min at 3000 ×*g*, the liquid supernatants of the samples were stored at −80 °C.

2.3. Methods

2.3.1. NOD procedure

In accordance with standard accepted indicators of depressive behavior [a huddled posture and decreased responsiveness to environmental stimuli (Shively et al., 2005)], three trained observers identified depressed subjects from among 6012 adult *Macaca fascicularis* after 2 weeks of behavioral observation. Sixteen female monkeys with the highest levels of depression-like behaviors were classified into the NOD group, while another 16 randomly selected healthy control female subjects (matched with the NOD animals for age) were assigned to the CON1 group. These animals underwent a 4-month period of observation (from April to August 2011). There were seven observation periods per day, each lasting 30 min. The daily observations were scheduled for the following times: A1: 10:00–10:30, A2: 10:30–11:00, A3: 11:00–11:30, A4: 14:30–15:00, A5: 15:00–15:30, A6: 15:30–16:00, and A7: 16:00–16:30, for which a Sony DCR-SR43 DV camera and focal observation were used (Li et al., 2013). More than 3.5 h of animal behavior was videotaped each day, for up to 120 observation days. Behavioral Frequencies and duration of behaviors were analyzed using Noldus software (version 10.0; Noldus Information Technology, Leesburg, PA). For each behavior measured, the consistency of rating among the three observers was determined to be > 85%.

2.3.2. *SVC procedure*

Twenty female macaques were randomly selected and blindly assigned to the SVC and CON2 groups. Prior to this study, the monkeys were raised together in the feeding base. The 10 CON2 subjects remained in the colony, while the 10 SVC subjects were transferred to separate cages (0.6 × 0.7 × 0.8 m) in a common room. The adaptation phase lasted for 14 d, following which the SVC monkeys were transferred to modified single cages (standard single cages with four blinds around them, such that the monkeys could hear or smell but not see the other monkeys). CON2 and SVC subjects, along with all other subjects, had free access to water and food, and were kept under a 12/12-h light/dark cycle (lights on 08:00–20:00). After 90 d of separation and continuous observation for 3 d, the animals in the SVC group were transferred back to the original colony.

2.3.3. *Behavior definition*

According to the “posture–location–action” rule, all behaviors were classified into 53 behavioral types and 12 categories. In this study, the behaviors were scored based on performance rate and time ratio (Xu et al., 2012a).

2.3.4. *Protein reduction, alkylation, and tryptic digestion*

After the acquisition of behavioral data, the CSF of each group of monkeys was pooled for the i-TRAQ (resulting in eight samples: NOD1 and NOD2, CON1-1 and CON1-2, SVC1 and SVC2, CON2-1 and CON2-2). The samples were concentrated to 100 μl by freezing. Ice-cold acetone was then added and the samples were precipitated overnight. After centrifugation at 14,000 ×*g* for 30 min, the precipitate was washed twice with 1 ml of pre-cooled acetone. The pellet was dissolved by adding 100 μl of UA (8 M urea, 150 mM TrisHCl; pH 8.0) buffer. Protein quantification was carried out by the Bradford method. Then, SDS-PAGE electrophoresis was performed. A total of 300 μg of protein from each group of samples was taken for enzymatic hydrolysis. DTT was added to a final concentration of 100 mM, after which the samples were boiled in water for 5 min and then cooled to room temperature. A total of 200 μl of UA buffer was added and mixed, and the solution was transferred to a 10 kDa ultrafiltration centrifuge tube. After centrifugation at 14,000 ×*g* for 15 min, the filtrate was discarded; this step was repeated twice. Then, 100 μl of IAA (50 mM IAA in UA) was added, and the solution was shaken at 600 rpm for 1 min, followed by incubation in the dark at room temperature for 30 min, and centrifugation at 14,000 ×*g* for 10 min. Next, 100 μl of UA buffer was added, followed by centrifugation at 14,000 ×*g* for 10 min; this step was repeated twice. A total of 40 μl of trypsin buffer (7 μg of trypsin in 40 μl of dissolution buffer) was added and the solution was shaken at 600 rpm for 1 min, followed by incubation at 37 °C for 16–18 h. The collection tube was then replaced, the solution was centrifuged at 14,000 ×*g* for 10 min, and the filtrate was collected. The peptide was then quantified using OD_{280} (Wiśniewski et al., 2009).

2.3.5. *i-TRAQ labeling and SCX fractionation*

A total of 100 μg of each sample was removed and labeled in accordance with the instructions of the i-TRAQ Reagent-8plex Multiplex Kit (AB SCIEX, Framingham,MASS USA). The labeling was performed as follows: CON1-1 labeled as 113, CON2-2 labeled as 114, NOD1 labeled as 115, NOD2 labeled as 116, SVC1 labeled as 117, SVC2 labeled as 118, CON2-1 labeled as 119, and CON2-2 labeled as 121 (with each group separated into two replicates). Each set of labeled peptides was mixed and subjected to strong cation exchange (SCX) prefractionation. Approximately 30 parts of the flowthrough and elution fractions were collected, and 20 parts were combined according to the SCX chromatogram. After lyophilization, the peptides were desalted with a C18 cartridge (66872-U; Sigma, St. Louis, MO, USA) [instrument: AKTA Purifier 100 (GE Healthcare, Chicago, IL, USA); column: polysulfoethyl 4.6 × 100 mm column (5 μm, 200 Å; PolyLC Inc., Columbia, MD, USA); buffers: Buffer A 10 mM KH_2PO_4 pH 3.0, 25% ACN, Buffer B 10 mM KH_2PO_4 pH 3.0, 500 mM KCl, 25% CAN] (Unwin et al., 2010).

2.3.6. *HPLC-MS/MS*

Each sample was separated by Easy nLC, a nanoliter flow rate HPLC liquid phase system. The following buffers were used: Solution A was 0.1% aqueous formic acid solution, and Solution B was 0.1% aqueous solution of formic acid in acetonitrile (84% acetonitrile). The column was equilibrated with 95% Solution A. The sample was loaded onto a Thermo Scientific EASY column (2 cm ×100 μm, 5 μm - C18) (Thermo Fisher Scientific, Waltham, MA, USA) and separated by another such column of a different size (75 μm × 100 mm, 3 μm - C18) at a flow rate of 300 nl/min by an autosampler. The relevant liquid-phase gradient was as follows: 0–50 min, Solution B linear gradient from 0% to 55%; 51–56 min, from 55% to 100%; and 56–60 min, maintenance at 100%.

Peptides separated by capillary HPLC were directly injected into a Q-Exactive mass spectrometer (Thermo Fisher Scientific), with positive ion mode and a selected mass range of 300–1800 mass/charge (m/z) for 60 min. First-order mass spectrometry parameters were as follows: resolution: 70,000 at m/z 200; AGC target: 3e6; first-level maximum IT: 10 ms; number of scan ranges: 1; and dynamic exclusion: 40.0 s. The mass-to-charge ratio of polypeptide fragments and polypeptides was collected as follows: 10 fragments of MS2 scan (activation type: HCD, isolation window: 2 m/z) collected after each full scan. Then, the secondary mass spectrometry parameters were as follows: resolution: 17,500 at m/z 200; microscans: 1; and secondary maximum IT: 60 ms. The normalized collision energy was 30 eV and the underfill ratio was set as 0.1%.

2.4. *Data analysis*

The raw file was retrieved using Maxquant 1.3.0.5 software, after which the library Mascot2.2 (version 2.2; Matrix Science, Boston, MA, USA) and Proteome Discoverer 1.4 (Thermo Fisher Scientific, Waltham, MA, USA) were used for library identification and quantitative analysis. The database was downloaded from UniProt (1. uniprot_human.fasta, including 133,549 sequences, downloaded on 3/3/2013; 2. uniprot_Macaca_ 101595_20150504, including 101,595 records, downloaded on 5/4/2015) and the “decoy” option was used to calculate the false discovery rate (FDR). The search parameters were set as follows: enzyme, trypsin; de-isotopic: true; max. missed cleavages: 2; fixed modifications: carbamidomethyl (C); variable modifications: oxidation (M); first search ppm: 20 ppm; main search ppm: 6 ppm; database pattern: reverse; min. reporter PIF: 0.75; peptide FDR ≤ 0.01; and protein FDR ≤ 0.01.

The peptide peak intensity values were reported by Proteome Discoverer 1.4 software. There were four sets of samples from cynomolgus monkeys, each consisting of two biological replicates. For quantification, the average value of the eight tag labels was used as the internal parameter, and the ratio of each tag label was the channel tag to the internal parameter. Then, the significance index (p-value) was calculated (Cox and Mann, 2008; Pi et al., 2015). Proteins filtered by applying the following thresholds were used for further analysis: p-value < 0.05 and 1.2-fold change (> 1.20 or < 0.80).

2.5. Proteomic function and pathway analyses

Gene Ontology (GO) annotation terms of cell components were determined from all identified proteins using the online tool DAVID (http://david.abcc.ncifcrf.gov). The Kyoto Encyclopedia of Genes and Genomes (KEGG; http://www.genome.jp/kegg/) was used for molecular function annotation. For biological function analysis, a diagram was plotted based on the proteins with the highest scores from both IPA and PPI analyses, generated using the CluePedia plugin of Cytoscape 3.6.1. Signaling pathway annotations and relevant networks for significantly differentially expressed proteins were generated using Ingenuity Pathway Analysis software (IPA; QIAGEN, Redwood City, CA, USA). IPA was introduced in 2003 and helps researchers to analyze omics data and model biological systems. STRING (https://string-db.org/) was used to describe the functional protein association networks. The PPI network was also plotted using Cytoscape.

2.6. Statistical analysis

All results are expressed as mean ± standard deviation (SD). Monkey body weights were analyzed by repeated-measures ANOVA with group as an independent factor and time as a repeated measure. For the behavioral observations, Student's *t*-test was used to analyze the significance of differences among the groups. All data management and statistical analyses were performed using Stata 22.0 (StataCrop LP, College Station, TX, USA) (Zhang et al., 2016). Fisher's exact test was used in functional analysis and network generation. The threshold for statistical significance in all analyses was set at $p < 0.05$.

3. Results

3.1. Characteristics of cynomolgus monkey groups

The characteristics of the depressed and nondepressed monkey groups are presented in Table 1. In terms of age and body weight, there were no differences between the SVC and CON2 groups [age ($p = 0.15$), weight ($p = 0.37$)] or between the NOD and CON1 groups [age ($p = 0.42$), weight ($p = 0.17$)].

3.2. NOD monkeys showed higher depression behavior scores than SVC monkeys

Based on the principle of posture–location–environment, Xu previously validated and classified 53 behaviors into 12 categories (Supplementary Table 1) to establish a behavioral spectrum of cynomolgus monkeys (Qin et al., 2016; Shively, 1998; Shively and Day, 2015; Shively et al., 2005). All behaviors in the study were sorted into the following behavioral categories: amicable, anxiety, resting, conflict, ingestion and drinking, thermoregulatory, rutting, locomotive, depression, and miscellaneous. The depressed subjects showed more anxiety, conflict, and depression behaviors (Table 2). First, NOD monkeys exhibited significantly higher scores for both the depression behaviors (i.e., "blinking," "contracture," "bowing") and the anxiety behaviors (i.e., "quickly itching," "locomotive") than the controls. Second, NOD subjects spent more time on ingesting, thermoregulatory, and locomotive behaviors than CON1, but not rutting. Here, ingestion refers to the licking of food residue scattered on the floor. More amicable behaviors were observed in the depression subjects than in the control monkeys, while the opposite trend was seen for the conflict behaviors. Between the SVC and CON2 groups, significant differences were observed in the scores for the "depression," "anxiety," "amicable," and "locomotive" behaviors.

3.3. i-TRAQ-based quantitative proteomic analysis of the CSF of NOD and SVC subjects vs. controls

Before the i-TRAQ-based quantitative proteomic analysis, SDS-PAGE was performed to identify the protein was not degraded (Supplementary Fig. 1). In total, in the NOD vs. CON1 and SVC vs. CON2 comparisons, 5032 unique peptides (909 protein groups) were identified and quantified. Each of the four sample groups (NOD group, CON1 group, SVC group, CON2 group) had two technical duplicates (Fig. 1 A). The average of the eight labels was defined as the internal reference, and the ratio of each label was the ratio between the label and the average.

The results showed that the distribution of the log2 (CON1-1/REF, CON1-2/REF) ratio could be fitted to a Gaussian curve with an SD of 0.09 & 0.07 ($n = 904$), that of the log2 (NOD1/REF,NOD2/REF) ratio could be fitted with an SD of 0.18 & 0.04 ($n = 904$), while the log2 (CON2-1/REF, CON2-2/REF) ratio could be fitted with an SD of 0.06 & 0.03 ($n = 903$); in addition, 902 proteins were quantified with an SD of 0.02/0.04 for the distribution of log2 (SVC1/REF, SVC2/REF) ratio (Fig. 1B). Using a minimum of two peptides for protein identification, in the NOD/CON1 chart, the expression levels of 40 proteins were changed in NOD, with 16 proteins being upregulated and 24 being downregulated. In the SVC/CON2 chart, 40 proteins changed expression, with 17 proteins being upregulated and 23 downregulated. Comparing the NOD group with the SVC group, 36 proteins showed a change of expression, with 23 proteins being upregulated and 13 downregulated. The results of cluster analysis for the differentially expressed proteins showed that SVC stress significantly altered the expression of some proteins compared with the levels in the control group and also the NOD group (Fig. 1C). The results of quantification of the differentially expressed proteins are shown in Supplementary Table 2.

3.4. Bioinformatic analysis revealed differential pathology associated with depression in NOD and SVC models

Next, the results of GO analysis for the proteins with altered expression in each group were submitted to a DAVID analysis, which included biological process, molecular function, and cellular component analyses. The results of GO analysis showed that glucose metabolic process, generation of precursor metabolites and energy, ATP binding, inflammatory response, immune response, extracellular region and homeostatic process, cytosol, and ion binding were particularly prominent in the NOD – CON1 group (Supplementary Fig. 2), SVC – CON2 group (Supplementary Fig. 2C), and NOD-SVC group (Supplementary

Table 1
The Group Data of Cynomolgus monkey.

Variable	NOD	CON1	P	SVC	CON2	P
Macaques Subjects (n)	16	16	NA	10	10	NA
Age (yr) *	12.20 ± 0.74	11.65 ± 1.90	0.42	12.20 ± 0.66	11.65 ± 1.90	0.15
weight (kg) *	5.81 ± 0.76	5.93 ± 0.88	0.17	5.55 ± 0.59	5.93 ± 0.88	0.37
Offspring	0	4	NA	0	4	NA

* Data presented as means ± S.D.'s. Student's *t*-test was used to analyze significant differences.

Table 2

Differential Behaviors in NOD Subjects and SVC Subjects.

Behavioral Item	NOD(S)	CON1(S)	P-value	SVC(S)	CON2(S)	P-value
Amicable behavior	118.18 ± 62.318	44.69 ± 25.520	.000***	48.20 ± 26.882	12.455 ± 3.939	.025*
Anxiety behavior	59.00 ± 41.688	9.50 ± 12.749	.000***	18.20 ± 15.992	3.10 ± 5.174	.016*
Rest behavior	1108.4 ± 56.896	1084.0 ± 76.772	.305	906.00 ± 75.122	892.50 ± 96.156	.731
Conflict behavior	33.29 ± 25.521	85.50 ± 39.433	.000***	40.70 ± 21.406	24.40 ± 17.771	.080
Ingestive behavior	163.71 ± 45.154	121.13 ± 66.652	.039*	74.60 ± 28.601	54.00 ± 24.545	.101
Thermo-regulatory behavior	110.88 ± 57.924	64.13 ± 14.881	.005**	99.00 ± 55.315	118.60 ± 32.582	.347
Rutting behavior	2.76 ± 1.855	5.06 ± 1.482	.000***	3.30 ± 2.163	2.90 ± 1.969	.671
Locomotive behavior	27.12 ± 19.368	122.25 ± 48.362	.000***	117.30 ± 40.045	63.90 ± 25.649	.002**
Depression behavior	21.35 ± 21.272	0.88 ± 1.025	.001**	34.90 ± 23.154	5.10 ± 6.871	.001**,
Miscellaneous behavior	56.29 ± 20.775	49.38 ± 16.852	.303	60.50 ± 17.251	59.40 ± 15.005	.881

Data listed as means ± SDs. Student's *t*-test was used to analyze significant differences.
*P < 0.05, ** P < 0.01, *** P < 0.001.

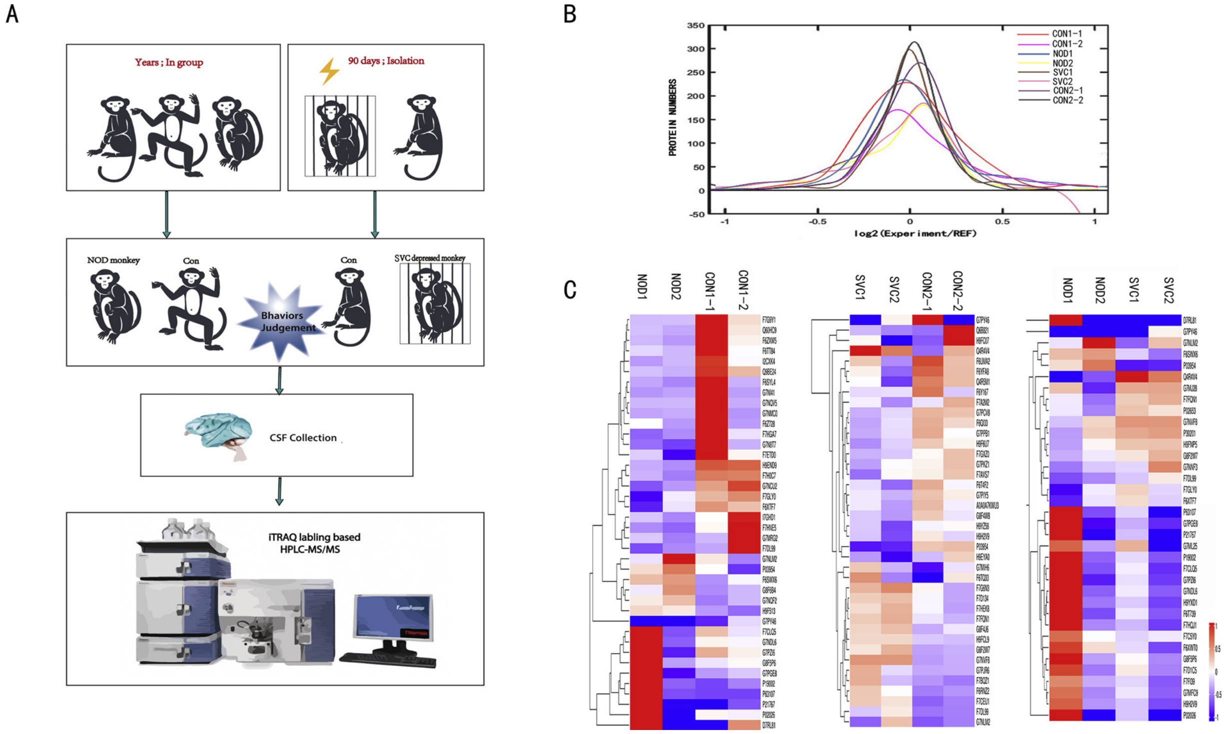

Fig. 1. Quantitative proteomic comparison of the cerebrospinal fluid (CSF) of naturally occurring depression (NOD) and social plus visual isolation-induced depression (SVC) subjects using the i-TRAQ approach. (A) Workflow of model establishment. (B) Histograms of log2 ratio distributions of quantified proteins: NOD1/REF, NOD2/REF (n = 904), CON1-1/REF, CON1-2/REF (n = 904), SVC1/REF, SVC2/REF (n = 902), and CON2-1/REF, CON2-2/REF (n = 903). (C) Hierarchical clustering of the differentially expressed proteins. Clustering was based on the expression levels of proteins analyzed by feature selection.

Fig. 2E). KEGG analysis showed that the proteins with altered expression in the NOD-CON1 group were particularly associated with glucose metabolism disorder (Fig. 2A), while the MAPK signaling pathway and focal adhesion were highlighted in the SVC – CON2 group (Fig. 2B). Using CluePedia for biological function analysis, the results showed that the differentially expressed proteins in the NOD – CON1 group were notably linked to the positive regulation of mitochondrial ATP synthesis – COupled proton transport, carbohydrate catabolic process, and hydrogen peroxide catabolic process (Supplementary Fig. 2B).

To uncover the functions of the differentially expressed proteins of each group, we used IPA for further analysis. Canonical pathways were examined first, with the top ten pathways shown. In the NOD group, the highest scores were for glycolysis I and gluconeogenesis I, and the next most affected pathways were calcium signaling, protein kinase A signaling, and actin cytoskeleton signaling (Fig. 2C). As expected, different pathways were identified for the SVC group, with the liver X receptor/retinoid X receptor (LXR/RXR) pathway and farnesoid X receptor/retinoid X receptor (FXR/RXR) pathways being most significantly affected (Fig. 2D). IPA was used to rank the differentially expressed proteins by the significance of their association, grouping the proteins into three categories: diseases and disorders, molecular and cellular functions, and physiological system development and function. In the category of diseases and disorders (Fig. 2E), hematological disease was the top-ranking function of NOD – CON1, while inflammatory response was for SVC – CON2. Other pertinent diseases such as neurological diseases, psychological disorders, and metabolic diseases were included in both groups. Significant changes in the expression level of components in these pathways and systems might lead to bio-functional changes and disease development. In the category of molecular and cellular functions (Fig. 2F), cellular assembly and organization, and cellular movement were the top-ranked in the NOD group, while protein synthesis and lipid metabolism were in the SVC group. One significantly disturbed network in the NOD – CON1 group was that related to carbohydrate metabolism, cellular assembly and organization, and cellular movement, which had a score of 62 (Fig. 2G) and had 21 dysregulated proteins (all downregulated). The highest scoring network

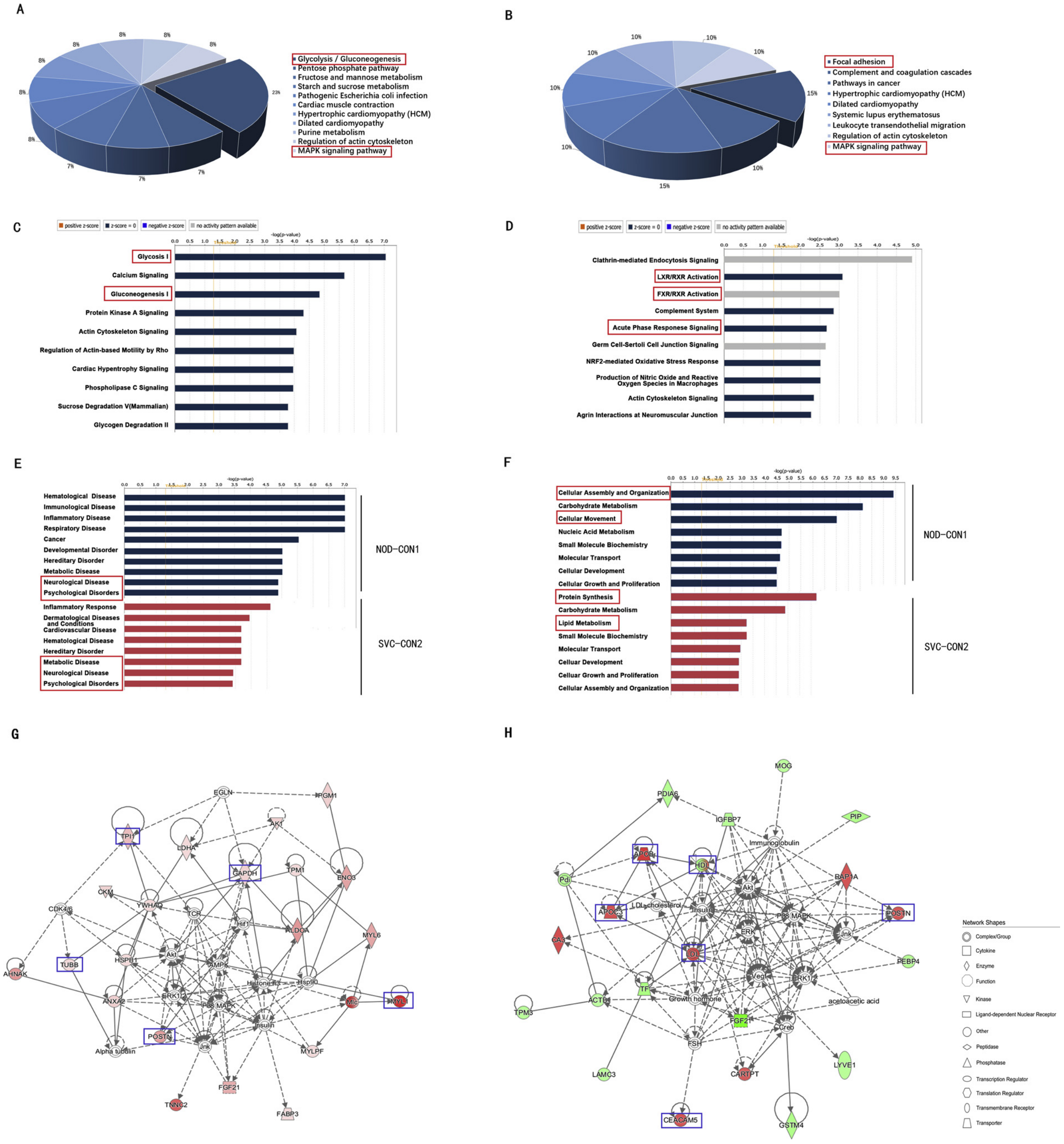

Fig. 2. Bioinformatic and network analysis for the differentially expressed proteins in the CSF of NOD and SVC subjects vs. controls by DAVID and IPA. (A) and (B) KEGG pathway analysis of 40 (NOD) and 40 (SVC) significantly differentially expressed proteins. (C) The 10 most prominent canonical pathways in NOD vs. CON1. (D) The 10 most prominent canonical pathways in SVC vs. CON2. (E) Disease and disorder. (D) Molecular and cellular functions. Networks clustered by IPA: (G) NOD vs. CON1, (H) SVC vs. CON2.

(with a score of 50) in SVC − CON2 was that involving response to protein synthesis, cardiovascular disease, and hematological disease (Fig. 2H).

The results of GO analyses (Supplementary Fig. 2E) and KEGG analyses for the proteins with altered expression between NOD and SVC depressed monkeys were also subjected to a DAVID analysis. Relationships with the LXR/RXR pathway, FXR/RXR pathway, IL-12 signaling, and production of nitric oxide and reactive oxygen species in macrophages were detected (Fig. 3A). Next, the protein–protein interaction (PPI) networks were analyzed using STRING (Supplementary Fig. 2F). CluePedia for biological function analysis of proteins from PPI networks showed clustering in association with the positive regulation of hydrogen peroxide catabolic process, metabolic processes, and negative regulation of lipid catabolic process in the comparison of NOD vs. SVC (Fig. 3B). These results also conversely showed a large difference between NOD and SVC.

The differences in the results observed for the NOD − CON1 group and the SVC − CON2 group indicate that distinct biological mechanisms might underlie naturally occurring depression and SVC-induced depression. For example, negative regulation of glucose energy metabolism was found to be important in the NOD subjects, while lipid metabolism was the top-ranking affected process in the SVC subjects.

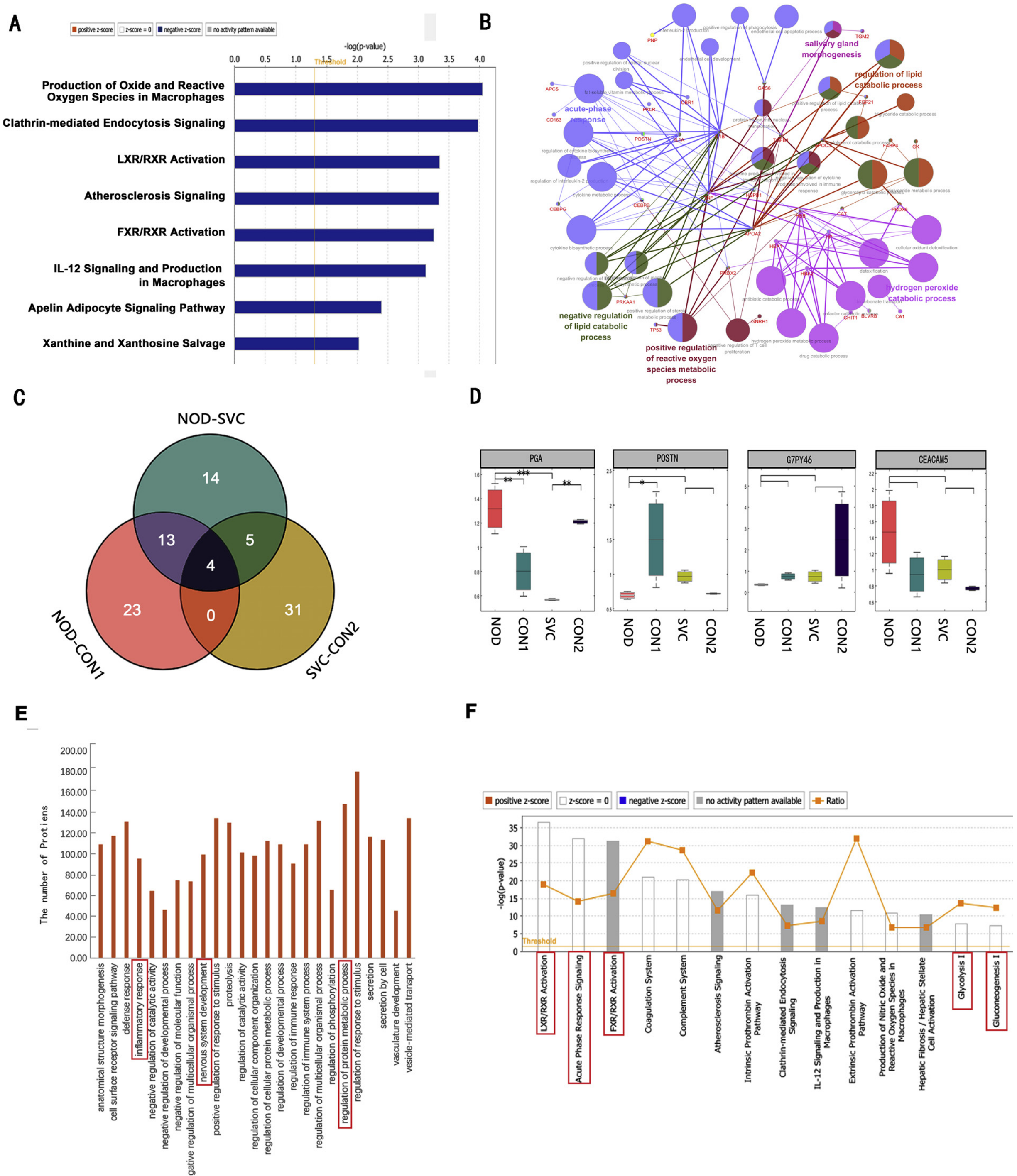

Fig. 3. Bioinformatic analysis of the differentially expressed proteins identified in CSF of NOD vs. SVC and depressed patients. (A) Pathway analysis of 36 significantly differentially expressed proteins of NOD vs. SVC by IPA. (B) Biological process of NOD vs. SVC was generated by Cytoscape. (C) Overlap of the proteins identified in NOD vs. CON1, SVC vs. CON2, and NOD vs. SVC; four common proteins are presented. (D) Expression of the four proteins in each group (NOD, CON1, SVC, and CON2). (E) Protein functional clustering of cerebrospinal fluid (CSF) from human major depressive disorder (MDD) patients. (F) A total of 152 identified differentially expressed proteins and their most strongly related canonical pathways.

3.5. Comparison of NOD and SVC indicated some similarities between the two models of depression

We found that there were four common dysregulated proteins among all three groups (NOD – CON1, SVC – CON2, NOD-SVC) (Fig. 3C). The results of quantification of the differentially expressed proteins are shown in Supplementary Table 3. The abundances of the four proteins in multivariate analysis for the three groups were analyzed. The abundances between the groups were compared using pairwise Mann–Whitney tests (*p < 0.05, **p < 0.01, ***p < 0.001; Fig. 3D).

3.6. Proteomic analysis of human CSF revealed that energy metabolism disturbance is involved in depression

We employed shotgun proteomics on the CSF collected from 16

MDD patients as a control before exposure to antidepressants and health examiner (demographic and clinical characteristics of the participants are shown in Supplementary Table 4). Patients with depression did not differ from the healthy controls in terms of age and gender ratio. SDS-PAGE was performed before proteomic analysis (Supplementary Fig. 1B). A total of 437 proteins were identified, of which 152 were differentially expressed between MDD and HC (shown in Supplementary Table 5). Classification of these 152 differentially expressed proteins by GO analysis indicated that they were particularly associated with inflammatory response, nervous system development, and regulation of protein metabolic processes (Fig. 3E). Furthermore, IPA classical signaling pathway analysis showed high scores for the RXR (retinoid X receptor) pathway and acute-phase response signaling. Surprisingly, it also showed significant correlation with glycolysis I and gluconeogenesis I (Fig. 3F).

3.7. Proteomic studies in rodents after CUMS revealed significant disorders of energy metabolism

Previously, we conducted i-TRAQ proteomic studies on brain regions and tissues of CUMS depression rodents (Cheng et al., 2016; Li et al., 2018, 2017; Rao et al., 2016; Shao et al., 2015; Yang et al., 2013). We identified disordered energy metabolism in the olfactory bulb, prefrontal cortex, cerebellum, hypothalamus, plasma, and liver of rodents (Fig. 4). Specific details and information on the identified molecular changes can be found in Supplementary Table 6.

4. Discussion

To our knowledge, this is the first study to investigate CSF proteomics of both naturally occurring depression and social plus visual isolation-induced depression in cynomolgus monkeys by i-TRAQ and a combined analysis with CSF data from human MDD patients. Our findings demonstrate significant diversification of energy metabolism in NOD and MDD patients. Early perturbation of lipid metabolism may be involved in the pathophysiology of MDD (Xu et al., 2012b), and was also found to play a role in SVC *Macaca fascicularis* and MDD patients in our study.

4.1. Adult female cynomolgus monkeys as NOD and SVC models used for in-depth research

We used cynomolgus monkeys (*Macaca fascicularis*) to describe and model a naturally occurring depressive state in a non-human primate species. The depressive state arose in a natural colony-based social environment, where social hierarchy produces stress-inducing social competition, with no experimental manipulation to disturb the etiological process. Moreover, to construct a social and visual isolation-induced depressed model, the monkeys were exposed to intense mental and psychological stimulation in a relatively short period of time (Li et al., 2013).

Both NOD model and SVC model monkeys exhibited depressive and anxiety-like behaviors. However, NOD model subjects showed less conflict behaviors (e.g., conflict avoidance, being scared, elude).

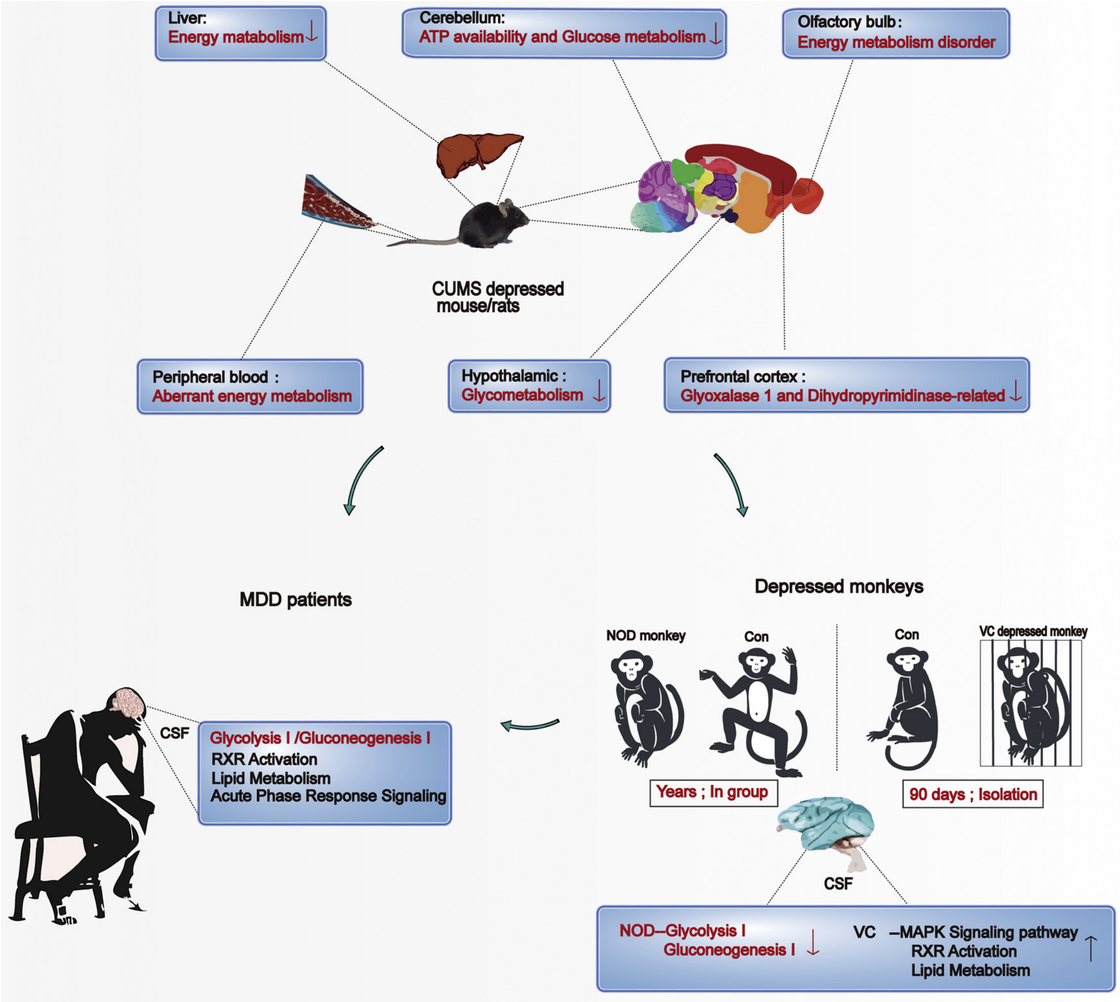

Fig. 4. Overview of disturbances of energy metabolism in depressed patients, rodents, and NOD/SVC cynomolgus monkeys.

Meanwhile, their amicable, rutting, and locomotive behaviors were significantly increased, while their ingestive behavior and thermoregulatory behavior increased slightly. There were no significant differences in these behaviors in the SVC model monkeys. These findings may be related to low social status in the group and low mood state (Shively, 1998). MDD patients show increased anxiety, shortage sexual behaviors. Low levels of motivation and low self-awareness are the main features of MDD patients (Kelly et al., 2012). The behavior of NOD model subjects more closely resembled that of human patients with chronic mild stress-induced depression. In the SVC model, depression and anxiety behaviors were most commonly observed. The SVC model effectively mimicked depressive behavior under severe but short-term social isolation stress.

The NOD and SVC models may reveal divergent pathways behind the induction of depression, which means that both NOD and SVC monkey models could play different but useful roles in the future study of emotion disorders.

4.2. Energy metabolism

In proteomic analysis of cerebrospinal fluid in human MDD, the differential expression of proteins involved in glycolysis I and gluconeogenesis I was identified. This is consistent with previous studies, which showed that, in a rodent model of chronic mild stress, energy metabolism disorders occurred in most brain regions and plasma and liver tissue (Cheng et al., 2016; Li et al., 2018, 2017; Rao et al., 2016; Shao et al., 2015; Yang et al., 2013). The energy metabolic pathways involved were glycolysis/gluconeogenesis, the tricarboxylic acid (TCA) cycle, and oxidative phosphorylation. The levels of related molecules such as glyceraldehyde-3-phosphate dehydrogenase (GAPDH), pyruvate kinase (PK), and lactate dehydrogenase (LDH) changed in the prefrontal cortex or cerebellum in response to the downregulation of glucose metabolism. Together with the up- or downregulation of diverse enzymes of the mitochondrial respiratory chain, it has also been suggested that ATP biosynthesis is disordered in MDD. Increased levels of enzymes involved in glycolysis and the TCA cycle further highlight perturbations of energy metabolism as one of the pathophysiological symptoms of depression.

In the current study, a number of proteins involved in glycolysis/gluconeogenesis were significantly downregulated in depressed subjects compared with the levels in controls, including triosephosphate isomerase 1 (TPI1), adenylate kinase 1 (AK1), aldolase, fructose-bisphosphate A (ALDOA), G3PDH, and LDH (Fig. 2G). TPI1 is an enzyme consisting of two identical proteins, which catalyzes the isomerization of G3PDH and dihydroxyacetone phosphate (DHAP) in glycolysis and gluconeogenesis. AK1 is an adenylate kinase enzyme involved in energy metabolism and homeostasis of cellular adenine nucleotide ratios in different intracellular compartments. Alteration of G3PDH was previously identified in the hippocampus and prefrontal cortex of depression rat models and upon treatment with antidepressants (Carboni et al., 2006; Kedracka-Krok et al., 2010; Mallei et al., 2011; Marais et al., 2009; Piubelli et al., 2011). Moreover, alteration of LDH was previously identified in the cerebellum of depression rat models (Shao et al., 2015). The activities of several key enzymes related to glucose metabolism were found to be reduced, leading to severe oxidative metabolic disorders, adenosine triphosphate reduction, and oxidative stress. Furthermore, a ternary protein complex comprising G3PDH, seven in absentia homolog 1, and Ras homolog, enriched in the brain and driven by nitric oxide, might be the molecular cascade responsible for the antidepressant-like effect of ketamine (Harraz and Snyder, 2017).

Some proteins related to ATP regulation or translation enzymes were found when we analyzed the proteins differentially expressed between NOD and controls, including ATP synthase subunit alpha (ATP5F1A), myosin light chain 1 (MYL1), and myosin light chain 6 (MYL6) (Fig. 2G and Supplementary Table 2). Recently, ATP has been found to be a key modulator of depressive-like behavior in adult mice, and bioenergetic dysfunction was also reported as a factor contributing to mental illnesses (Cao et al., 2013). Moreover, neuroimaging studies also revealed alterations in biomarkers for energy metabolism; specifically, reduced ATP availability and reductions in glucose metabolism were observed in the brains of MDD patients (Baxter et al., 1989; Iosifescu and Renshaw, 2003). Downregulation of these proteins may reduce energy metabolism by downregulating glucose transport, thereby increasing the susceptibility to depression.

4.3. Inflammatory reaction and lipid metabolism

In the bioinformatic analysis of proteins associated with SVC depression, these were shown to be involved in the MAPK pathway, with 23 dysregulated proteins being involved in inflammatory responses. Interestingly, IL12 signaling and acute-phase response signaling stood out as high-scoring canonical pathways in the MDD proteomic analysis (Fig. 3F). Consistent with our findings, inflammation has been shown to be involved in the pathophysiology and treatment response of major depressive disorder (MDD). A study has also shown a broad effect of depression on the immune system, with MDD patients exhibiting elevated levels of six pro-inflammatory cytokines: IL-12, TNF, IL-6, IFNγ, IL-9, and IL-17A (Syed et al., 2018).

The results of the current study, together with the changes of CYP2A4 and SULT2A1 in the liver of CUMS rodent models (Wu et al., 2016), provide strong evidence for the effects of lipid metabolism on the pathogenesis of depression. IPA analysis of SVC model monkeys showed that “LXR/RXR activation,” a key pathway of lipid metabolism, was the best matched pathway in the CSF of subjects with SVC depression. Previous proteomic analyses of CSF from MDD patients found similar results. Overall, lipid metabolism may thus play a latent role in depression.

4.4. Potential biomarkers

Bioinformatic/proteomic analysis revealed four common differentially expressed proteins in CSF between the two primate depression-like models: PGA, POSTN, G7PY46, and CEACAM5. The same trends of change of G7PY46 and CEACAM5 were found in both NOD − CON1 and SVC − CON2.

Carcinoembryonic antigen (CEA) is known to accompany signs of immune-inflammatory responses in bipolar disorder (BD) and medical disorders [Bulut, 2019 #1287][Bulut, 2019 #1287](Bulut et al., 2019). CEACAM5 is not only involved in cell adhesion, intracellular signaling, and tumor progression, but has also been found to be a receptor for *Escherichia coli*, which has a major effect on neuropsychiatric diseases (Korotkova et al., 2008; Oikawa et al., 1989). Regarding G7PY46, this exerts growth factor activity, but has not been well characterized. In this case of PGA, this encodes Pepsin A-1, which is upregulated in NOD − CON1 (FC = 1.64) but downregulated in SVC − CON2 (FC = 0.47). Pepsin A-1 plays an important role in aspartyl protease, hydrolase, and protease activities, suggesting that the TCA cycle might be affected by it. Conversely, POSTN encodes Periostin, which was upregulated in SVC − CON2 (FC = 1.34) but downregulated in NOD − CON1 (FC = 0.46). Periostin is a matricellular protein that has been implicated in many diseases, and was recently reported as a biomarker of type 2 inflammation (Izuhara et al., 2016). Identification of the inverse changes of PGA and POSTN might not only be suitable for depression classification and diagnosis, but also meaningful for distinguishing NOD models from SVC ones.

Although CSF is used for clinical diagnosis, this approach can be invasive and inaccurate; novel biomarkers could be very useful in diagnosing MDD, which currently still relies on subjective evaluation and clinical examinations (Hacimusalar and Eşel, 2018; Lo and Huang, 2018; Woods et al., 2014). Given the difference of sensitivity to various drugs in patients with MDD, CSF-based biomarkers might be useful for diagnosis and treatment, and provide meaningful evidence and medication guidance, following further research.

4.5. *Differential pathways to depression*

In this study, we primarily provided overall CSF protein profiles of two cynomolgus monkey models of depression and compared them with each other. Following bioinformatic analysis, inflammatory response, energy metabolism, lipid metabolism dysregulation, MAPK signaling pathway, and RXR activation were identified as differing significantly between them. The present proteomic analysis of CSF from MDD patients also showed perturbed energy metabolism, specifically in glycolysis/gluconeogenesis and lipid metabolism. Comparison of the CSF proteins of human MDD patients with those of NOD model monkeys demonstrated the similarities in glycolysis/gluconeogenesis dysregulation in these two species. The NOD model might thus be uniquely suited to research on the involvement of energy metabolism in the pathogenesis of MDD. Meanwhile, the strong consistency of alterations in the inflammatory process and lipid metabolism between the SVC model and MDD patients also warrants further investigation, to obtain a better understanding of MDD’s pathophysiology and to identify novel therapeutic targets.

There are many different pathways to depression in humans. We hypothesize that, under mild and chronic stimulation, the pathway to depression might occur via disordered glucose metabolism; in contrast, under rapid and strong stress stimulation and social isolation, it could mainly involve disruption of lipid metabolism and immune inflammation.

The differences and similarities of i-TRAQ proteomics in CSF between NOD and SVC models provide new evidence for the correlation between depression and energy metabolism, and provide better models for the future study of mechanisms of depression and for guiding clinical drug application and treatment.

4.6. *Limitations*

There are some limitations to this study, as follows: (1) Not all differentially expressed proteins could be classified in the analyses with DAVID, IPA, and Cytoscape because of limitations of the protein databank of *Macaca fascicularis*. (2) In addition, the total number of included subjects was small, so the results may not be generalizable. Additional studies are needed to overcome these issues, and to clarify the dysregulated proteins’ specific roles in mediating pathways and signaling cascades. (3) Furthermore, no biological duplication was performed, although this is required to reinforce our results. (4) Finally, the heterogeneity of two models both genetically and physiologically could also not be controlled. The effects of genetic factors on promoting depression were not considered.

5. Declarations of interest

The authors have declared no conflict of interest in the submission of this manuscript.

Acknowledgments

This work was financially supported by the National Basic Research Program of China (Grant No. 2017YFA0505700), the National Natural Science Foundation of China (Grant No. 81601207 and 81701361), and The Project of Science and Technology of Chongqing Yuzhong District (20170113). We are grateful to Shanghai Applied Protein Technology Compony for supporting the proteomics technology. We also thank Melony Black, PhD, from Liwen Bianji, Edanz Editing China (www.liwenbianji.cn/ac), for editing the English text of a draft of this manuscript.

Appendix A. Supplementary data

Supplementary material related to this article can be found, in the online version, at doi:https://doi.org/10.1016/j.psyneuen.2019.05.007.

References

Bai, S., Li, W., Zhou, C., Zheng, P., Fang, L., Wang, H., Liu, Y., Xie, P., 2018. Urinary biomarker panel for diagnosing patients with depression and anxiety disorders.%A Chen JJ. Transl. Psychiatry 8, 192.

Baxter Jr., L.R., Schwartz, J.M., Phelps, M.E., Mazziotta, J.C., Guze, B.H., Selin, C.E., Gerner, R.H., Sumida, R.M., 1989. Reduction of prefrontal cortex glucose metabolism common to three types of depression. Arch. Gen. Psychiatry 46, 243–250.

Brent, D.A., Brunwasser, S.M., Hollon, S.D., Weersing, V.R., Clarke, G.N., Dickerson, J.F., Beardslee, W.R., Gladstone, T.R., Porta, G., Lynch, F.L., Iyengar, S., Garber, J., 2015. Effect of a cognitive-behavioral prevention program on depression 6 years after implementation among At-Risk adolescents: a randomized clinical trial. JAMA Psychiatry 72, 1110–1118.

Bulut, M., Cati, S., Gunes, M., Kaya, M.C., Kaplan, I., Ozkan, M., 2019. Evaluation of serum inflammatory markers in treatment-resistant manic patients and adequate responder manic patients. Psychiatry Res. 272, 73–79.

Cao, X., Li, L.P., Wang, Q., Wu, Q., Hu, H.H., Zhang, M., Fang, Y.Y., Zhang, J., Li, S.J., Xiong, W.C., Yan, H.C., Gao, Y.B., Liu, J.H., Li, X.W., Sun, L.R., Zeng, Y.N., Zhu, X.H., Gao, T.M., 2013. Astrocyte-derived ATP modulates depressive-like behaviors. Nat. Med. 19, 773–777.

Carboni, L., Piubelli, C., Pozzato, C., Astner, H., Arban, R., Righetti, P.G., Hamdan, M., Domenici, E., 2006. Proteomic analysis of rat hippocampus after repeated psychosocial stress. Neuroscience 137, 1237–1246.

Cheng, K., Li, J., Yang, D., Yang, Y., Rao, C., Zhang, S., Wang, W., Guo, H., Fang, L., Zhu, D., Han, Y., Xie, P., 2016. 2D-gel based proteomics unravels neurogenesis and energetic metabolism dysfunction of the olfactory bulb in CUMS rat model. Behav. Brain Res.

Cox, J., Mann, M., 2008. MaxQuant enables high peptide identification rates, individualized p.p.b.-range mass accuracies and proteome-wide protein quantification. Nat. Biotechnol. 26, 1367–1372.

Cui, Y., Sang, K., Dong, Y., Ni, Z., Ma, S., Hu, H., 2018. Ketamine blocks bursting in the lateral habenula to rapidly relieve depression.%A Yang Y. Nature 554, 317–322.

Fox, A., Shelton, S., Rogers, J., Dyer, T., Davidson, R., Shelledy, W., Oakes, T., Blangero, J., Kalin, N., 2010. Amygdalar and hippocampal substrates of anxious temperament differ in their heritability.%A Oler JA. Nature 466, 864–868.

Gomez, R., Williams, G., Lembke, A., Lazzeroni, L., Murphy, G., Schatzberg, A., 2017. HPA axis in major depression: cortisol, clinical symptomatology and genetic variation predict cognition.%A Keller J. Mol. Psychiatry 22, 527–536.

Guo, K., Zeng, L., Zeng, B., Huo, R., Luo, Y., Wang, H., Dong, M., Zheng, P., Zhou, C., Chen, J., Liu, Y., Liu, Z., Fang, L., Wei, H., Xie, P., 2018. Metabolite identification in fecal microbiota transplantation mouse livers and combined proteomics with chronic unpredictive mild stress mouse livers.%A Li B. Transl. Psychiatry 8, 34.

Hacimusalar, Y., Eşel, E., 2018. Suggested biomarkers for major depressive disorder. Noro Psikiyatr. Ars. 55, 280–290.

Harraz, M.M., Snyder, S.H., 2017. Antidepressant actions of ketamine mediated by the mechanistic target of rapamycin, nitric oxide, and rheb. Neurotherapeutics 14, 728–733.

Iosifescu, D.V., Renshaw, P.E., 2003. 31P-magnetic resonance spectroscopy and thyroid hormones in major depressive disorder: toward a bioenergetic mechanism in depression? Harv. Rev. Psychiatry 11, 51–63.

Izuhara, K., Conway, S.J., Moore, B.B., Matsumoto, H., Holweg, C.T., Matthews, J.G., Arron, J.R., 2016. Roles of periostin in respiratory disorders. Am. J. Respir. Crit. Care Med. 193, 949–956.

Kedracka-Krok, S., Fic, E., Jankowska, U., Jaciuk, M., Gruca, P., Papp, M., Kusmider, M., Solich, J., Debski, J., Dadlez, M., Dziedzicka-Wasylewska, M., 2010. Effect of chronic mild stress and imipramine on the proteome of the rat dentate gyrus. J. Neurochem. 113, 848–859.

Kelly, R.E., Mansell, W., Sadhnani, V., Wood, A.M., 2012. Positive and negative appraisals of the consequences of activated states uniquely relate to symptoms of hypomania and depression. Cogn. Emot. 26, 899–906.

Korotkova, N., Yang, Y., Le Trong, I., Cota, E., Demeler, B., Marchant, J., Thomas, W.E., Stenkamp, R.E., Moseley, S.L., Matthews, S., 2008. Binding of Dr adhesins of Escherichia coli to carcinoembryonic antigen triggers receptor dissociation. Mol. Microbiol. 67, 420–434.

Laber-Laird, K., Anton, R., 1997. Behavior and physiology of social stress and depression in female cynomolgus monkeys.%A shively CA. Biol. Psychiatry 41, 871–882.

Li, X., Xu, F., Xie, L., Ji, Y., Cheng, K., Zhou, Q., Wang, T., Shively, C., Wu, Q., Gong, W., Fang, L., Zhan, Q., Melgiri, N.D., Xie, P., 2013. Depression-like behavioral phenotypes by social and social plus visual isolation in the adult female Macaca fascicularis. PLoS One 8, e73293.

Li, J., Zhang, S.X., Wang, W., Cheng, K., Guo, H., Rao, C.L., Yang, D.Y., He, Y., Zou, D.Z., Han, Y., Zhao, L.B., Li, P.F., Xie, P., 2017. Potential antidepressant and resilience mechanism revealed by metabolomic study on peripheral blood mononuclear cells of stress resilient rats. Behav. Brain Res. 320, 12–20.

Li, B., Guo, K., Zeng, L., Zeng, B., Huo, R., Luo, Y., Wang, H., Dong, M., Zheng, P., Zhou, C., Chen, J., Liu, Y., Liu, Z., Fang, L., Wei, H., Xie, P., 2018. Metabolite identification in fecal microbiota transplantation mouse livers and combined proteomics with chronic unpredictive mild stress mouse livers. Transl. Psychiatry 8, 34.

Liu, L., Zhou, X., Zhang, Y., Pu, J., Yang, L., Yuan, S., Zhao, L., Zhou, C., Zhang, H., Xie, P., 2018. Hippocampal metabolic differences implicate distinctions between physical and psychological stress in four rat models of depression. Transl. Psychiatry 8, 4.

Lo, L., Huang, T.-L., 2018. Proteomics approach for biomarker research in major depression: antidepressant effects. Curr. Drug Metab. 19, 502–512.

Loh, Y., Purushothaman, I., Walker, D., Parise, E., Salery, M., Cahill, M., Hodes, G., Pfau, M., Kronman, H., Hamilton, P., Issler, O., Labonté, B., Symonds, A., Zucker, M., Zhang, T., Meaney, M., Russo, S., Shen, L., Bagot, R., Nestler, E., 2018. Estrogen receptor α drives pro-resilient transcription in mouse models of depression.%A Lorsch ZS. Nat. Commun. 9, 1116.

Mallei, A., Giambelli, R., Gass, P., Racagni, G., Mathe, A.A., Vollmayr, B., Popoli, M., 2011. Synaptoproteomics of learned helpless rats involve energy metabolism and cellular remodeling pathways in depressive-like behavior and antidepressant response. Neuropharmacology 60, 1243–1253.

Marais, L., Hattingh, S.M., Stein, D.J., Daniels, W.M., 2009. A proteomic analysis of the ventral hippocampus of rats subjected to maternal separation and escitalopram treatment. Metab. Brain Dis. 24, 569–586.

Oikawa, S., Inuzuka, C., Kuroki, M., Matsuoka, Y., Kosaki, G., Nakazato, H., 1989. Cell adhesion activity of non-specific cross-reacting antigen (NCA) and carcinoembryonic antigen (CEA) expressed on CHO cell surface: homophilic and heterophilic adhesion. Biochem. Biophys. Res. Commun. 164, 39–45.

Pi, E., Qu, L., Hu, J., Huang, Y., Qiu, L., Lu, H., Jiang, B., Liu, C., Peng, T., Zhao, Y., Wang, H., Tsai, S.-N., Ngai, S., Du, L., 2015. Mechanisms of soybean roots' tolerances to salinity revealed by proteomic and phosphoproteomic comparisons between two cultivars. MCP 15.

Piubelli, C., Carboni, L., Becchi, S., Mathe, A.A., Domenici, E., 2011. Regulation of cytoskeleton machinery, neurogenesis and energy metabolism pathways in a rat gene-environment model of depression revealed by proteomic analysis. Neuroscience 176, 349–380.

Qin, D.D., Rizak, J., Feng, X.L., Yang, S.C., Lu, L.B., Pan, L., Yin, Y., Hu, X.T., 2016. Prolonged secretion of cortisol as a possible mechanism underlying stress and depressive behaviour. Sci. Rep. 6, 30187.

Rao, C., Shi, H., Zhou, C., Zhu, D., Zhao, M., Wang, Z., Yang, Y., Chen, J., Liao, L., Tang, J., Wu, Y., Zhou, J., Cheng, K., Xie, P., 2016. Hypothalamic proteomic analysis reveals dysregulation of glutamate balance and energy metabolism in a mouse model of chronic mild stress-induced depression. Neurochem. Res. 41, 2443–2456.

Reynolds, R., Masiulis, I., Eisch, A., 2016. Re-evaluating the link between neuropsychiatric disorders and dysregulated adult neurogenesis.%A Yun S. Nat. Med. 22, 1239–1247.

Shao, W.H., Chen, J.J., Fan, S.H., Lei, Y., Xu, H.B., Zhou, J., Cheng, P.F., Yang, Y.T., Rao, C.L., Wu, B., Liu, H.P., Xie, P., 2015. Combined metabolomics and proteomics analysis of major depression in an animal model: perturbed energy metabolism in the chronic mild stressed rat cerebellum. OMICS 19, 383–392.

Shively, C.A., 1998. Social subordination stress, behavior, and central monoaminergic function in female cynomolgus monkeys. Biol. Psychiatry 44, 882–891.

Shively, C.A., 2011. Social stress and cardiovascular disease in Primates. Stress and Cardiovascular Disease 17–29 chapter2.

Shively, C.A., Day, S.M., 2015. Social inequalities in health in nonhuman primates. Neurobiol. Stress 1, 156–163.

Shively, C.A., Williams, J.K., Laber-Laird, K., Anton, R.F., 2002. Depression and coronary artery atherosclerosis and reactivity in female cynomolgus monkeys. Psychosom. Med. 64, 699–706.

Shively, C.A., Register, T.C., Friedman, D.P., Morgan, T.M., Thompson, J., Lanier, T., 2005. Social stress-associated depression in adult female cynomolgus monkeys (Macaca fascicularis). Biol. Psychol. 69, 67–84.

Syed, S.A., Beurel, E., Loewenstein, D.A., Lowell, J.A., Craighead, W.E., Dunlop, B.W., Mayberg, H.S., Dhabhar, F., Dietrich, W.D., Keane, R.W., de Rivero Vaccari, J.P., Nemeroff, C.B., 2018. Defective inflammatory pathways in Never-Treated depressed patients are associated with poor treatment response. Neuron 99, 914–924 e913.

Tsuchimine, S., Kunugi, H., 2018. Cerebrospinal fluid monoamine metabolite concentrations in depressive disorder: a meta-analysis of historic evidence.%A Ogawa S. J. Psychiatr. Res. 105, 137–146.

Unwin, R., Griffiths, J., Whetton, A., 2010. Simultaneous analysis of relative protein expression levels across multiple samples using iTRAQ isobaric tags with 2D nano LC-MS/MS. Nat. Protoc. 5, 1574–1582.

van Dammen, L., Leeflang, M., Limpens, J., Roseboom, T., de Rooij, S., 2018. Hypothalamic-pituitary-adrenal axis and autonomic nervous system reactivity in children prenatally exposed to maternal depression: a systematic review of prospective studies.%A Bleker LS. Neurosci. Biobehav. Rev undefined: undefined.

Voleti, B., Hajszan, T., Rajkowska, G., Stockmeier, C., Licznerski, P., Lepack, A., Majik, M., Jeong, L., Banasr, M., Son, H., Duman, R., 2012. Decreased expression of synapse-related genes and loss of synapses in major depressive disorder.%A Kang HJ. Nat. Med. 18, 1413–1417.

Wisniewski, J.R., Zougman, A., Nagaraj, N., Mann, M., 2009. Universal sample preparation method for proteome analysis. Nat. Methods 6, 359–362.

Woods, A.G., Iosifescu, D.V., Darie, C.C., 2014. Biomarkers in major depressive disorder: the role of mass spectrometry. Adv. Exp. Med. Biol. 806, 545–560.

Wu, Y., Tang, J., Zhou, C., Zhao, L., Chen, J., Zeng, L., Rao, C., Shi, H., Liao, L., Liang, Z., Yang, Y., Zhou, J., Xie, P., 2016. Quantitative proteomics analysis of the liver reveals immune regulation and lipid metabolism dysregulation in a mouse model of depression. Behav. Brain Res. 311, 330–339.

Xu, F., Xie, L., Li, X., Li, Q., Wang, T., Ji, Y., Kong, F., Zhan, Q., Cheng, K., Fang, L., Xie, P., 2012a. Construction and validation of a systematic ethogram of Macaca fascicularis in a free enclosure. PLoS One 7, e37486.

Xu, H.B., Zhang, R.F., Luo, D., Zhou, Y., Wang, Y., Fang, L., Li, W.J., Mu, J., Zhang, L., Zhang, Y., Xie, P., 2012b. Comparative proteomic analysis of plasma from major depressive patients: identification of proteins associated with lipid metabolism and immunoregulation. Int. J. Neuropsychopharmacol. 15, 1413–1425.

Xu, F., Wu, Q., Xie, L., Gong, W., Zhang, J., Zheng, P., Zhou, Q., Ji, Y., Wang, T., Li, X., Fang, L., Li, Q., Yang, D., Li, J., Melgiri, N.D., Shively, C., Xie, P., 2015. Macaques exhibit a naturally-occurring depression similar to humans. Sci. Rep. 5, 9220.

Yang, Y., Yang, D., Tang, G., Zhou, C., Cheng, K., Zhou, J., Wu, B., Peng, Y., Liu, C., Zhan, Y., Chen, J., Chen, G., Xie, P., 2013. Proteomics reveals energy and glutathione metabolic dysregulation in the prefrontal cortex of a rat model of depression. Neuroscience 247, 191–200.

Zeng, B., Zeng, L., Du, X., Li, B., Huo, R., Liu, L., Wang, H., Dong, M., Pan, J., Zheng, P., Zhou, C., Wei, H., Xie, P., 2018. Gut microbiota regulates mouse behaviors through glucocorticoid receptor pathway genes in the hippocampus.%A Luo Y. Transl. Psychiatry 8, 187.

Zhang, S., Wang, W., Li, J., Cheng, K., Zhou, J., Zhu, D., Yang, D., Liang, Z., Fang, L., Liao, L., Xie, P., 2016. Behavioral characterization of CD36 knockout mice with SHIRPA primary screen. Behav. Brain Res. 299, 90–96.